Soluble model involving four identical particles*

A. C. Fonseca† and P. E. Shanley
Department of Physics, University of Notre Dame, Notre Dame, Indiana 46556
(Received 14 May 1976)

Using a nonrelativistic field theoretic formalism, a soluble model of scattering involving four identical spinless particles is developed and solved numerically. In addition to the elementary "nucleon" (the n), two composite particles meant to approximate the deuteron and triton are introduced with the couplings $d \leftrightarrow n + n$ and $t \leftrightarrow d + n$. By consistently excluding all particle-exchange contributions to the three-body sector, four-body integral equations are obtained for the two-to-two processes: $nt \rightarrow nt$, $nt \rightarrow dd$ as well as for $dd \rightarrow dd$ and $dd \rightarrow nt$. Numerical solutions of the equations are found to satisfy unitarity constraints above the two-, three-, and four-body thresholds. The positions of the four-body bound states are obtained and a complete phase shift calculation is performed. The sum of the total three- and four-body breakup cross sections predicted by the model are displayed as a function of energy and the angular distributions for all $2 \rightarrow 2$ reactions are compared with the four-nucleon data.

[NUCLEAR REACTIONS Four-body problem. Spinless model of the four-nucleon system.]

I. INTRODUCTION

Over the past several years, the general features of the bound state and scattering properties of the three-nucleon system have been successfully described by surprisingly simple potential models of the two-nucleon interaction.[1] This success may be attributed to the long-range nature of the underlying nucleon-exchange mechanism that lessens the need for a sophisticated two-particle interaction. While it is reassuring that the theoretical description of the three-nucleon system is being carried out correctly, a disadvantage of this lack of sensitivity is that two-nucleon information is difficult to obtain from the three-nucleon observables. If we shift our consideration to the four-nucleon system, a more complicated set of exchange mechanisms should prevail, involving both one-nucleon exchange and also correlated as well as uncorrelated two-nucleon exchange. It would be expected that in the four-nucleon system these processes lead to an interaction of shorter range and thus that the observables would depend more sensitively on the two-particle force. As evidence for this one could point to the large binding energy of the α particle. In this paper we introduce a soluble model of the four-nucleon system in an attempt to study this question as well as others.

Although formally correct integral equations exist for the four-body problem,[2] their complexity is so great that no scattering solutions exist for a realistic nucleon-nucleon interaction. Most of the calculations that have been performed involve bound state[3] or threshold scattering[4] results and the use of a separable two-nucleon interaction. Bound state results for a Yukawa potential[5] are also available as well as scattering calculations[6] involving propagator approximations in the four-body equations.

In a recent paper[7] we introduced an exactly soluble four-body model involving two pairs of identical particles and we now adapt this model to a spinless version of the four-nucleon system. In our previous work, restrictions on the interactions allowed between the particles led to one-dimensional four-body integral equations that are readily solved numerically. This simplicity was largely due to the lack of particle-exchange contributions to the three-body sector of the model. In our present problem with four identical particles, all pairs are coupled by the same two-body force and particle-exchange contributions are present at the three-body level since the dynamical equation is that of the Amado model.[8] For the four-nucleon system we find it necessary to insert an approximation for the three-body amplitude by introducing a quasiparticle with the coupling $t \leftrightarrow d + n$ and retain only direct-channel contributions to nd elastic scattering. The resulting three-body amplitude is separable and nd scattering proceeds exclusively through the spinless t. With this approximation we obtain four-body integral equations for the processes $nt \rightarrow nt$ and $nt \rightarrow dd$ as well as for $dd \rightarrow dd$ and $dd \rightarrow nt$. After partial wave decomposition they reduce to single variable equations that can be readily solved numerically. Although our approximation involves the neglect of certain classes of graphs, detailed numerical calculations have shown that the total cross sections obtained from unitarity for $2 \rightarrow 3$ processes in the three-body sector and for $2 \rightarrow 3$ and $2 \rightarrow 4$ processes

in the four-body sector are non-negative and thus we find that our three-body approximation leads to no gross violation of unitarity.

In spite of the simplicity of the model and the absence of spin, we were tempted to compare our results with the four-nucleon data. The angular distributions resulting from the exact solution of our equations are capable of reproducing the data within the same order of magnitude, particularly at higher energies where the absence of spin is less important. In nt elastic scattering the cross section presents a backward peak characteristic of an exchange mechanism and the forward peak is reasonably well reproduced. The position and number of the four-body bound states have also been obtained. For the maximum value of the coupling constants two s-wave bound states are found. By decreasing the coupling, the higher bound state disappears and with a small variation of the parameters of the model the α-particle binding energy can be fitted.

In Sec. II we introduce the two- and three-body amplitudes of the model. The four-body equations for elastic and rearrangement processes are obtained in Sec. III. In Sec. IV we present the results of the numerical calculations and in Sec. V some discussion and conclusions are given.

II. TWO- AND THREE-BODY SCATTERING

In the two-body sector of the model, our interaction is the same as that in the Amado model. We allow only the s-wave coupling $d \rightarrow n+n$ as depicted in Fig. 1. Elastic nn scattering proceeds through the d and this process can be described in terms of a non-relativistic unrenormalized Hamiltonian ($\hbar^2 = 2m_n = 1$)

$$H_d = \sum_{\vec{k}} \vec{k}^2 N^\dagger(\vec{k}) N(\vec{k}) + \sum_{\vec{k}} (-\epsilon_d^{(0)} + \tfrac{1}{2}\vec{k}^2) D^\dagger(\vec{k}) D(\vec{k}) + \left[\frac{\gamma_d^{(u)}}{2} \sum_{\vec{q}\vec{Q}} f_d(\vec{q}) D^\dagger(\vec{Q}) N(\tfrac{1}{2}\vec{Q} - \vec{q}) N(\tfrac{1}{2}\vec{Q} + \vec{q}) + \text{H.c.} \right], \tag{1}$$

where N and D are annihilation operators suitable for bosons, $\vec{q}$ and $\vec{Q}$ are the relative and total momenta of the two interacting particles, and $\epsilon_d^{(0)}$ is the bare binding energy of the d. The two-body scattering amplitude resulting from (1) has been graphically represented in Fig. 2(a) and has a separable form in momentum space

$$\langle \vec{k}' | T_{nn}(E) | \vec{k} \rangle = \tfrac{1}{2}\gamma_d^2 f_d(\vec{k}) \tau_d(E + \epsilon_d) f_d(\vec{k}') , \tag{2}$$

where τ_d is the d-particle propagator shown in Fig. 2(b). The interaction is characterized by a coupling constant γ_d and a vertex function $f_d(\vec{q})$ as well as a wave function renormalization constant Z_d that is allowed to take on the range of values $0 \leq Z_d \leq 1$. If $Z_d = 1$, the d is an elementary particle uncoupled to $n+n$, while if $Z_d = 0$, a separable potential model is obtained in which the d is a bound state of two n's. The specific form of the d-particle propagator and conversion to conventional units are discussed in Appendix A.

If we move to the three-body sector with the interaction generated by (1), nd scattering proceeds by successive n exchanges and the scattering amplitude satisfies the integral equation shown pictorially in Fig. 3. In each partial wave l, the equation reads

$$T_l(k', k; E) = B_l(k', k; E) + \frac{1}{2\pi^2} \int_0^\infty n^2 dn\, B_l(k', n; E) \times \tau_d(E + \epsilon_d - \tfrac{3}{4}n^2) T_l(n, k; E) , \tag{3}$$

where B_l is the single n-exchange Born term and

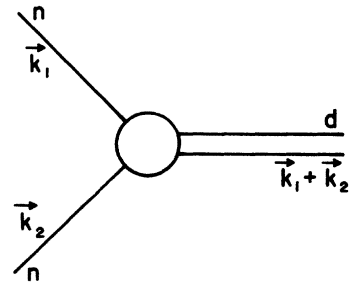

FIG. 1. Basic vertex for $d \rightarrow n + n$.

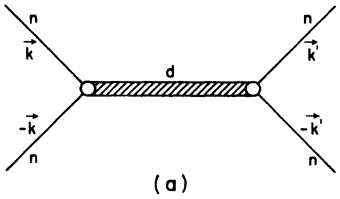

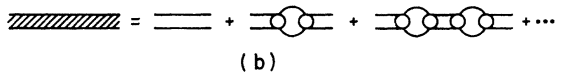

FIG. 2. (a) Graphical representation of the nn scattering amplitude. (b) First few terms in an expansion of the d-particle propagator.

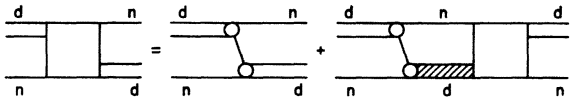

FIG. 3. Graphical representation of the integral equation for the $nd \rightarrow nd$ amplitude (square) as described by the Amado model.

τ_d is the d propagator. The predictions of this three-body model involving the numerical solution of (3) have been extensively discussed by Aaron, Amado, and Yam.[9]

To proceed to the four-body problem with no further approximation would lead to the numerical difficulties inherent in multivariable integral equations, so that we insert our three-body approximation at this point. We assume that the three-body problem of interest contains one bound state and that the nd scattering amplitude is dominated by the s-wave pole. We therefore introduce an extra spinless particle t with the s-wave coupling $t \rightarrow d+n$ as shown in Fig. 4. In analogy to the previous case, we can generate this process with the following interaction Hamiltonian:

$$H_t^I = \gamma_t^{(u)} \sum_{\vec{q}\vec{Q}} f_t(\vec{q}) T^\dagger(\vec{Q}) D(\vec{Q}\tfrac{2}{3} - \vec{q}) N(\vec{Q}\tfrac{1}{3} + \vec{q}) + \text{H.c.}\,. \quad (4)$$

If we were to allow both interactions $d \rightarrow n+n$ and $t \rightarrow d+n$ to all orders in each coupling, we could still obtain an amplitude for $nd \rightarrow nd$ in closed form[10] which consists of two parts. The first being nd scattering not involving the t which is just the process shown in Fig. 3 and the second part involves all graphs that proceed through an intermediate t. Our aim is not to study this more general amplitude, but to formulate a simplified three-body amplitude for use in the four-body sector of the model. We construct our approximate amplitude by considering the subclass of graphs shown in Fig. 5(a) that involve intermediate t's as well as nd bubbles in intermediate states. The nd scattering now proceeds exclusively in s wave through the t and the three-body amplitude has a separable form in momentum space

$$\langle \vec{k}' | T_{nd}(E) | \vec{k} \rangle = \gamma_t^2 f_t(\vec{k}') \tau_t(E + \epsilon_t) f_t(\vec{k}) \,, \quad (5)$$

where τ_t is the t-particle propagator depicted in Fig. 5(b) whose construction will be left for Appendix B. The amplitude T_{nd} is characterized by a coupling constant γ_t, a vertex function $f_t(\vec{k})$, as well as a wave function renormalization constant

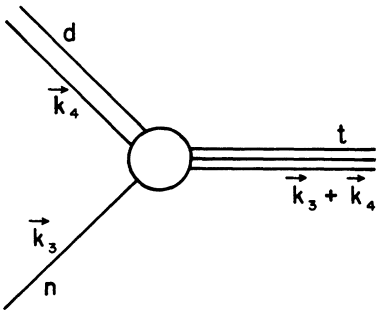

FIG. 4. Basic vertex for $t \rightarrow d+n$.

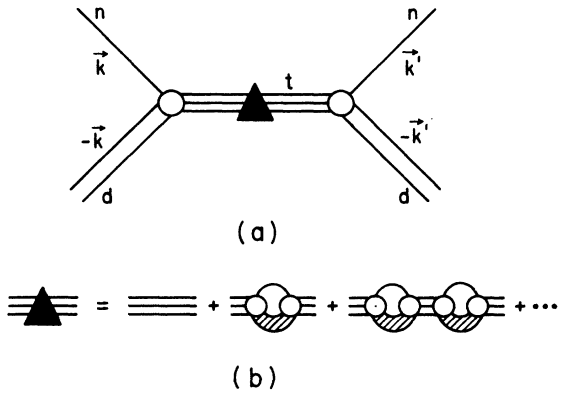

FIG. 5. (a) Graphical representation of the approximate amplitude for $nd \rightarrow nd$. (b) First few terms in an expansion of the approximate t-particle propagator.

Z_t. Since three-body intermediate states have been included in the propagator, our amplitude allows the process $nd \rightarrow nnn$ and therefore contains inelastic effects. We could also disallow this possibility by taking $Z_d = 1$ (elementary d). If in addition we take $Z_t = 0$, we would then have a model involving an effective separable potential between n and d with no breakup possible. Typical results obtained by the numerical evaluation of Eq. (5) are displayed in Fig. 6 where we show the

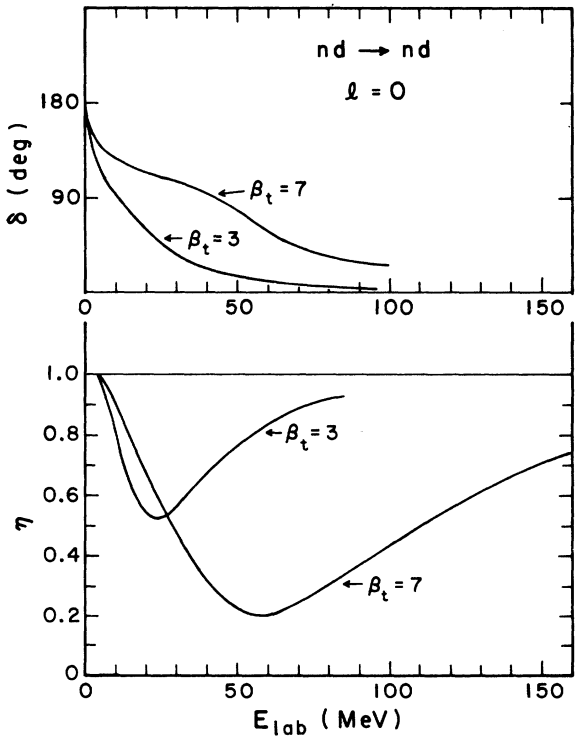

FIG. 6. δ and η versus E_n resulting from the solution of Eq. (5) for $nd \rightarrow nd$ with $Z_d = Z_t = 0$ and $\beta_d = 3.04$.

elastic s-wave nd phase shift δ and the inelastic parameter η as functions of energy. As suggested by Levinson's theorem we find that the real part of the s-wave phase shift δ decays monotonically from π to zero for $Z_d = Z_t = 0$. The inelastic parameter η has the value unity below the three-body threshold and remains between zero and one above the breakup threshold. For sufficiently high energy, η returns to unity.

It may appear surprising that no unitarity violation was observed in our three-body amplitude even though certain classes of graphs were neglected. In Fig. 7 we indicate some of the omitted contributions and these include n-particle exchange leading to $t \to d+n$ vertex corrections, as well as n-particle exchange inside the n-d bubbles. Also omitted were all processes in which nd scattering proceeds by multiple n exchange not involving the t as shown in Fig. 3. The complete mixing of the three n's implied by their identity is dynamically carried out by these n-particle-exchange contributions and we are thereby breaking the complete Bose symmetry of the system by neglecting these graphs. In our approximate amplitude, as graphically depicted in Fig. 5(a), the intermediate states are such that the two n's in the d bubbles are effectively uncoupled from the remaining n and thus the final n emerging from $nd \to nd$ is precisely the same n that entered initially and no replacement by the n's in the d is possible. The initial or final n particle is therefore not being treated on an equal footing with the n's in the d and instead could be considered as a distinguishable particle (the n'). We find that the total $2 \to 3$ cross section obtained from the optical theorem, is in fact identical to that predicted by a model in which we study $n'd \to n'd$ and $n'd \to n'nn$ in the presence of the interactions $d \to n+n$ and

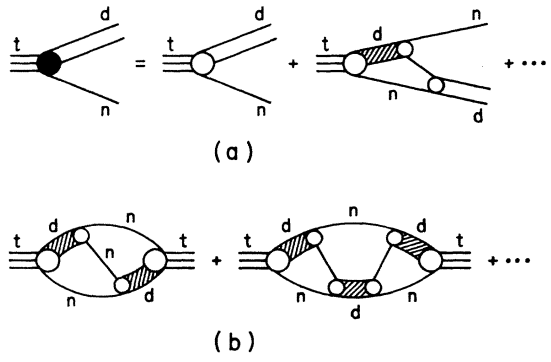

FIG. 7. (a) First few terms contributing to the nd vertex correction. Only the first term of the series was retained in our approximation. (b) Particle-exchange diagrams contributing to the t-particle propagator that have been omitted from consideration.

$t \to d+n'$.[7] This is an exact model since none of the omitted processes noted above is allowed. If we choose identical dynamic and kinematic parameters for both models, then the amplitude for $n'd \to n'd$ is functionally equal to the amplitude given in Eq. (5) for $nd \to nd$. Thus we see that our approximate three-body model does not violate unitarity because it is isomorphic to an exact and therefore unitary model.

III. FOUR-BODY SCATTERING

Having introduced an explicit field coupled to $n+d$ that led to a three-body amplitude in a separable form, we now proceed to the four-body sector and consider all two-particle-to-two-particle amplitudes. The possible reactions are $nt \to nt$ and $nt \to dd$ as well as $dd \to dd$ and $dd \to nt$. The simplifying assumption adopted in the three-body sector of the model is carried through in the four-body sector; that is, virtual nd scattering can occur only through the intermediate t. The four-body equations that we obtain here are therefore similar to the ones developed in a previous paper,[7] although some changes are necessary due to the identity of the four particles.

We want our four-body equations for the required processes to be of the Lipmann-Schwinger type where we have the product of well identified terms, that is, Born terms, intermediate propagators, and T matrices. As we have previously noted,[7] the presence of quasiparticle-quasiparticle states as off-shell external lines makes it difficult to separate the Born terms from the intermediate propagators. We will therefore construct our four-body equations in such a way that the quasiparticle-quasiparticle state dd never appears as an off-shell external line. Concentrating first on the reactions initiated by the nt state, a graphical representation of the integral equation for the $nt \to nt$ amplitude is illustrated in Fig. 8(a). The d-particle-exchange Born term and three box amplitudes are the inhomogeneous terms in the equation. Letting T_1 represent the full $nt \to nt$ amplitude, the specific form of the integral equation is

$$\langle \vec{k}' | T_1(E) | \vec{k} \rangle = \langle \vec{k}' | B(E) | \vec{k} \rangle + \int \frac{d^3n}{(2\pi)^3} \langle \vec{k}' | B(E) | \vec{n} \rangle \times \tau_t(E + \epsilon_t - \tfrac{4}{3}\vec{n}^2) \langle \vec{n} | T_1(E) | \vec{k} \rangle , \quad (6)$$

$$\langle \vec{k}' | B(E) | \vec{k} \rangle = \langle \vec{k}' | B_1(E) | \vec{k} \rangle + \langle \vec{k}' | \Box_1(E) | \vec{k} \rangle + \langle \vec{k}' | \Box_2(E) | \vec{k} \rangle .$$

$B_1(E)$ corresponds to the d-particle-exchange Born term, $\Box_1(E)$ to the box amplitude depicted first in Fig. 8(b), and $\Box_2(E)$ to the sum of the last

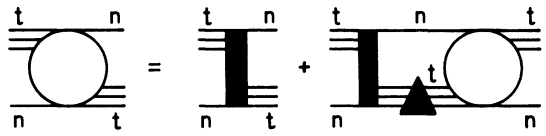

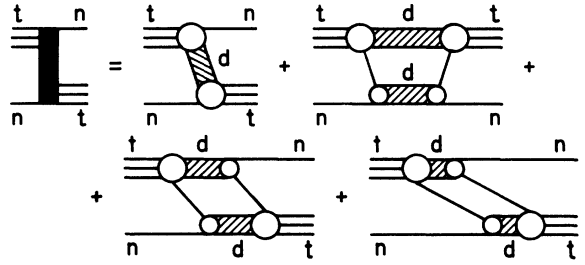

FIG. 8. Graphical representation of the integral equation for the $nt \to nt$ amplitude (circle).

two box amplitudes. The presence of two types of box amplitudes as inhomogeneous terms in the equation is due to the identity of the particles in the intermediate quasiparticle-quasiparticle state. Both $\Box_1(E)$ and $\Box_2(E)$ correspond to two-step processes in which an n particle is exchanged twice, the difference depending on whether the second exchange originates from the lower or from the upper d particle. In the latter case two situations can arise depending on whether the lower d is formed before or after the breakup of the upper d. While the Born term $B_1(E)$ describes the exchange of two correlated and fully interacting particles, the box amplitudes involve the exchange of two uncorrelated particles in a two-step process. The importance of these two-step processes to nt elastic scattering will be discussed later in Sec. IV. The solution of Eq. (6) also provides a means of obtaining the rearrangement amplitude for $nt \to dd$. Graphically this amplitude is represented in Fig. 9 where we see that it may be written in terms of an integral over the half-off-shell elastic amplitude $T_1(E)$. Letting T_2 be the amplitude for $nt \to dd$, the precise form of this relation is

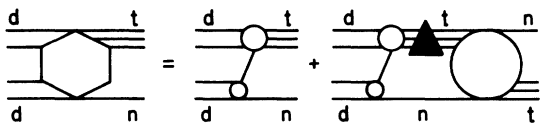

FIG. 9. Graphical representation of the integral relation expressing the $nt \to dd$ amplitude (hexagon) in terms of the half-on-shell $nt \to nt$ amplitude (circle).

$$\langle \vec{k}' | T_2(E) | \vec{k} \rangle = \langle \vec{k}' | B_2(E) | \vec{k} \rangle + \int \frac{d^3n}{(2\pi)^3} \langle \vec{k}' | B_2(E) | \vec{n} \rangle \times \tau_t(E + \epsilon_t - \tfrac{4}{3}\vec{n}^2) \langle \vec{n} | T_1(E) | \vec{k} \rangle , \quad (7)$$

where $B_2(E)$ is the single-particle-exchange Born term connecting nt to dd.

Having written the equations for the required $2 \to 2$ amplitudes initiated by the nt state, we must now calculate the Born terms $B_1(E)$ and $B_2(E)$ as well as the box amplitudes $\Box_1(E)$ and $\Box_2(E)$. $B_2(E)$ is the simplest and we only quote the result:

$$\langle \vec{k}' | B_2(E) | \vec{k} \rangle = \frac{\gamma_t \gamma_d}{\sqrt{2}} \left[\frac{f_t(\vec{k}' - \vec{k}\tfrac{2}{3}) f_d(\vec{k} - \tfrac{1}{2}\vec{k}')}{E + \epsilon_d - \tfrac{1}{2}\vec{k}'^2 - (\vec{k} - \vec{k}')^2 - \vec{k}^2} + \frac{f_t(\vec{k}' + \vec{k}\tfrac{2}{3}) f_d(\vec{k} + \tfrac{1}{2}\vec{k}')}{E + \epsilon_d - \tfrac{1}{2}\vec{k}'^2 - (\vec{k} + \vec{k}')^2 - \vec{k}^2} \right] , \quad (8)$$

where $\vec{k}$ and $\vec{k}'$ are the initial and final center of mass momenta, respectively. The presence of a direct and an exchange term in $B_2(E)$ is due to the identity of the particles in the dd state. The calculation of the d-particle-exchange Born term $B_1(E)$ is also straightforward and the result is

$$\langle \vec{k}' | B_1(E) | \vec{k} \rangle = \gamma_t^2 f_t(\vec{k}' + \tfrac{1}{3}\vec{k}) \tau_d(U) f_t(\vec{k} + \tfrac{1}{3}\vec{k}') , \qquad U = E + \epsilon_d - \vec{k}^2 - \tfrac{1}{2}(\vec{k} + \vec{k}')^2 - \vec{k}'^2 , \quad (9)$$

where $\vec{k}$ and $\vec{k}'$ are the center of mass momenta of the initial and final state. τ_d is the full d-particle propagator and thus $B_1(E)$ contains both the d-particle-exchange pole as well as the n-n continuum contribution.

The remaining task is to construct the box amplitudes $\Box_1(E)$ and $\Box_2(E)$, and this is done by a convolution procedure that has been discussed elsewhere.[7] We therefore will present here just the final results:

$$\langle \vec{k}' | \Box_i(E) | \vec{k} \rangle = \int \frac{d^3k''}{(2\pi)^3} \frac{\gamma_t \gamma_d f_t(\vec{k}'' + \vec{k}\tfrac{2}{3}) f_d(\vec{k} + \tfrac{1}{2}\vec{k}'')}{E + \epsilon_d - \tfrac{1}{2}\vec{k}''^2 - (\vec{k} + \vec{k}'')^2 - \vec{k}^2} G_i(\vec{k}, \vec{k}'', \vec{k}'; E) \frac{\gamma_d \gamma_t f_t(\vec{k}'' \pm \vec{k}''\tfrac{2}{3}) f_d(\vec{k}' \pm \tfrac{1}{2}\vec{k}'')}{E + \epsilon_d - \tfrac{1}{2}\vec{k}''^2 - (\vec{k}' \pm \vec{k}'')^2 - \vec{k}'^2} , \quad (10)$$

where the plus sign corresponds to $\Box_1(E)$ and the minus sign to $\Box_2(E)$. The G_1 and G_2 propagators are defined as

$$G_1(\vec{k},\vec{k}'',\vec{k}';E)=\tau_d(Y)-\frac{(Y-U)(Y-U')}{\pi}\int_0^\infty dx\frac{\mathrm{Im}[\tau_d(x+\epsilon_d)]}{(Y-U-\epsilon_d-x)}\frac{\tau_d(Y-\epsilon_d-x)}{(Y-U'-\epsilon_d-x)}, \tag{11}$$

$$G_2(\vec{k},\vec{k}'',\vec{k}';E)=\frac{Y-U''}{-U''}\tau_d(Y)+\frac{(Y-U)(Y-U'')}{Y-U-U''}\tau_d(U'')\tau_d(Y-U'')$$
$$-\frac{(Y-U)(Y-U'')}{\pi}\int_0^\infty dx\frac{\mathrm{Im}[\tau_d(x+\epsilon_d)]\tau_d(Y-\epsilon_d-x)}{(x+\epsilon_d-U'')(Y-U-\epsilon_d-x)}, \tag{12}$$

where

$$\begin{aligned}
Y&=E+\epsilon_d+\epsilon_d-\tfrac{1}{2}\vec{k}''^2-\tfrac{1}{2}\vec{k}''^2,\\
Y-U&=E+\epsilon_d-\tfrac{1}{2}\vec{k}''^2-(\vec{k}''+\vec{k})^2-\vec{k}^2,\\
Y-U'&=E+\epsilon_d-\tfrac{1}{2}\vec{k}''^2-(\vec{k}''+\vec{k}')^2-\vec{k}'^2,\\
Y-U''&=E+\epsilon_d-\tfrac{1}{2}\vec{k}''^2-(\vec{k}''-\vec{k}')^2-\vec{k}'^2.
\end{aligned} \tag{13}$$

Both propagators have a very complicated analytic structure since they contain two-, three-, and four-body effects resulting from the propagation of two quasiparticles.

At this point we have completed the construction of the dynamical equations for the $2\to2$ reactions initiated by the nt state. We now present the equations for an incoming dd state. Since the dd state is a quasiparticle-quasiparticle state we cannot establish an integral equation for the elastic scattering amplitude $dd\to dd$ as we did for $nt\to nt$, because this would require dealing with the quasiparticle-quasiparticle state as an off-shell external line. We first obtain an integral equation for $dd\to nt$ and the elastic amplitude is then calculated by performing an integration over the half-off-shell amplitude for $dd\to nt$. Naming T_3 the amplitude for $dd\to nt$, the specific form of the integral equation is

$$\langle\vec{k}'|T_3(E)|\vec{k}\rangle=\langle\vec{k}'|B_2(E)|\vec{k}\rangle+\int\frac{d^3n}{(2\pi)^3}\langle\vec{k}'|B(E)|\vec{n}\rangle\tau_t(E+\epsilon_t-\tfrac{4}{3}\vec{n}^2)\langle\vec{n}|T_3(E)|\vec{k}\rangle, \tag{14}$$

where $B_2(E)$ is given by Eq. (8) and $B(E)$ is the sum of $B_1(E)$, $\square_1(E)$, and $\square_2(E)$ given by Eqs. (9) and (10). Finally, letting T_4 be the amplitude for $dd\to dd$, the precise form of the integral relation between T_3 and T_4 is

$$\langle\vec{k}'|T_4(E)|\vec{k}\rangle=\int\frac{d^3n}{(2\pi)^3}\langle\vec{k}'|B_2(E)|\vec{n}\rangle\tau_t(E+\epsilon_t-\tfrac{4}{3}\vec{n}^2)\langle\vec{n}|T_3(E)|\vec{k}\rangle. \tag{15}$$

This terminates the description of our four-body equations for four identical spinless particles.

IV. RESULTS

As was previously pointed out it is our aim to solve on a computer the equations proposed in Sec. III for elastic and rearrangement scattering, to study the results as a function of the parameters of the model, and ultimately to apply it to the four-nucleon system. Our integral equations contain one vector variable in intermediate states and reduce to single variable equations following partial wave analyses. The singularity structure of the Born terms and box diagrams, though more complicated, is similar to that encountered in the three-body problem and the usual contour rotation method,[11] together with matrix inversion, has been used. The numerical calculations are straightforward but lengthy mainly due to the complicated analytic structure of the box amplitudes. This time restriction severely limited the study of the model as a function of the parameters, particularly in the scattering region. Using a 16 point integral equation mesh, the IBM 370/158 computer takes approximately 17 min to solve the equations for the three independent amplitudes in six partial waves.

The parametrization of the model is discussed in greater detail in Appendixes. The n-n interaction proceeds through the d and is characterized by three independent parameters: the binding energy of the d particle ϵ_d, the wave function renormalization constant Z_d, and β_d the range parameter of the vertex function $f_d(q)$. The n-d interaction proceeds exclusively through the t and is also characterized by another set of three parameters: ϵ_t, Z_t, and β_t. We have fixed ϵ_d and ϵ_t, respectively, at the deuteron and triton binding energies and in our units this corresponds to $\epsilon_d=0.5$ and $\epsilon_t=1.9047$.

A. Bound states

Here we examine the position and number of bound states by obtaining the zeros of the

Fredholm determinant $D_l(E)$ of Eq. (6) or (14). A zero of $D_l(E)$ below any scattering threshold is taken to imply a four-body bound state at that energy. We find such zeros only for $l=0$ and in Fig. 10 we display $D_0(E)$ versus E for various choices of Z_d with $Z_t=0$ and $\beta_d=\beta_t=4.0$. For $Z_d=0$ we also present the results for $D_1(E)$ and $D_2(E)$. Any variation of Z_d away from zero weakens the two-body n-n interaction and this results in a lower four-body binding energy. In the limit of $Z_d=1$, that is, no n-n interaction, we still obtain a bound state as a consequence of the field theoretic nature of the model where an elementary d can still interact with an n even in the absence of any n-n coupling. If we increase Z_t away from zero, the n-d interaction also becomes weaker and a lower binding energy for the four-body system is also obtained. In the limit of both Z_d and Z_t equal to zero, we encounter two s-wave four-body bound states. The effect of varying both Z_d and Z_t on the s-wave bound states is shown in Fig. 11 for fixed $\beta_d=\beta_t=4.0$. The upper bound state quickly disappears either by varying Z_d or Z_t away from zero. For the maximum value of the couplings ($Z_d=Z_t=0$) the ground state binding energy is 580 MeV and the excited state is bound by 13.6 MeV. The value we find for the binding energy of the four-body ground state is extremely unrealistic not only compared to the α-particle binding energy but also with respect to the values that have been obtained in previous calculations.[3] Such an effect in our model results from the kernel of the integral equations becoming independent of energy in the limit of large E for $Z_d=Z_t=0$. When $Z_d=0$, the d-exchange Born term loses its energy dependence at large E and similarly if $Z_t=0$, τ_t reduces to a constant for large E. This behavior results in a very slow convergence of the Fredholm determinant to unity as $E\to-\infty$ leading to an anomalously large ground state binding energy. We should note, however, that if the $t\to nd$ vertex corrections were included properly, the dressed vertex function would be energy dependent and presumably cure these difficulties. If Z_d or Z_t are changed away from zero, the α-particle binding energy can be fitted with a small adjustment of parameters. In fact, with $Z_d=Z_t=0.2$, $\beta_d=2.12$, and $\beta_t=5.0$ the four-body ground state becomes 28.4 MeV and no excited state is present.

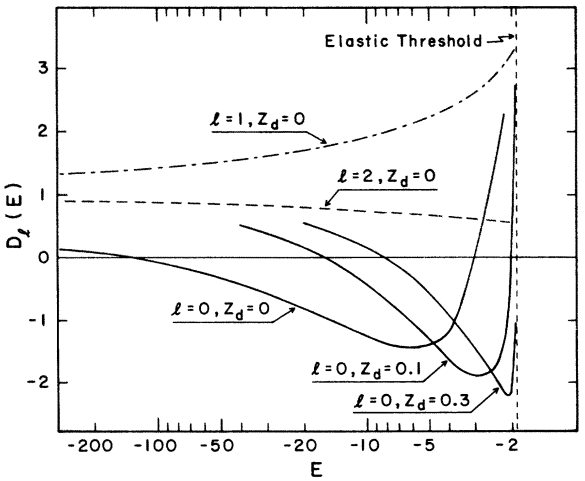

FIG. 10. Four-body Fredholm determinant $D_0(E)$ (solid line) versus E for $\beta_d=\beta_t=4.0$, $Z_t=0$, and several values of Z_d. The dashed line and the dash-dotted line represent $D_2(E)$ and $D_1(E)$, respectively, for the same set of parameters and $Z_d=0$. The energy units are such that the binding energy of the deuteron is $\epsilon_d=0.5$ and $\hbar^2=2m_n=1$ (see Appendix A).

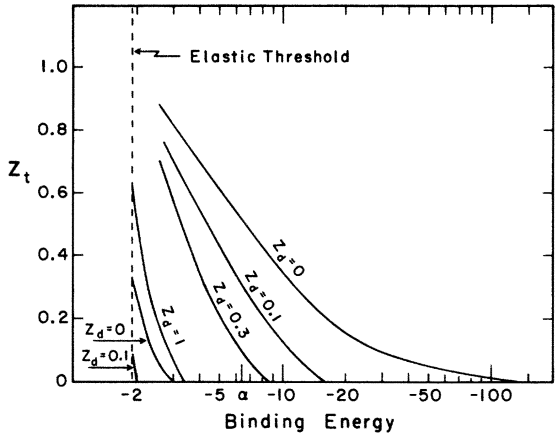

FIG. 11. Four-body binding energy versus Z_t for $\beta_d=\beta_t=4.0$ and several values of Z_d. The energy units are the same as in Fig. 10.

B. Scattering

The possible reactions and their energy thresholds are listed in Table I for the nt initial state. The numerical solution of the equations (6) and (7) for $nt\to nt$ and $nt\to dd$ yields the real and imaginary parts of the T matrix from which phase shifts and associated quantities can be constructed.

TABLE I. List of all possible reactions and their energy threshold for an nt initial state. The energy units are such that the binding energy of the deuteron is $\epsilon_d=0.5$ and $\hbar^2=2m_n=1$ (see Appendix A).

Reaction	Threshold
$nt\to nt$	$E=-1.9047$
$nt\to dd$	$E=-1.0$
$nt\to dnn$	$E=-0.5$
$nt\to 4n$	$E=0$

To fix the elastic phase shift at threshold we have adopted the convention suggested by Levinson's theorem and taken $\delta_l(0) = n\pi$, where n is the number of bound states present in the particular partial wave. In Fig. 12 we show the real part of the phase shift δ and inelastic parameter η for the s, p, and d waves contributing to $nt \to nt$ where $Z_d = Z_t = 0$ and $\beta_d = \beta_t = 4.0$. The real part of the s-wave phase shift falls from 2π at threshold to zero at infinity. The rate of decay varies and seems to be related to the position and depth of the minimum of the inelastic parameter η_0. For p waves, as well as for all other odd partial waves, the phase shift is negative due to the exchange nature of the n-t interaction and to the absence of the dd channel. In Fig. 13 we show the elastic phase shifts for $dd \to dd$ for the same set of parameters. Due to the identity of particles, only even partial waves are present. By varying Z_d or Z_t away from zero the $nt \to nt$ s-wave phase shift eventually changes its value at threshold to π when the upper bound state disappears. Both in $nt \to nt$ and $dd \to dd$ we find that the inelastic parameter η_l satisfies the constraint $0 < \eta_l \leq 1$ everywhere in the scattering region. This indicates that unitarity has not been grossly violated in spite of the approximate nature of our three-body amplitude. The total cross section obtained from the optical theorem is always greater than the sum of both total elastic and rearrangement cross sections, and the difference represents the total breakup cross sections for the $2 \to 3$ and $2 \to 4$ processes predicted by the model. In Figs. 14 and 15 we show the total cross sections for all processes. The sum of the total breakup cross sections for the $2 \to 3$ and $2 \to 4$ processes seems to agree reasonably well with the experimental values reported in a recent publication[12] where the total reaction cross section for the $p + {}^3\mathrm{He}$ interaction was measured for different values of the proton energy. For example, at 40 MeV the measured value is 115 mb, to be compared with 103 mb predicted by our model. The close agreement of the results is probably not significant due to the nonexistence of a dd channel in the $p - {}^3\mathrm{He}$ system and to the absence of spin and isospin effects in our calcula-

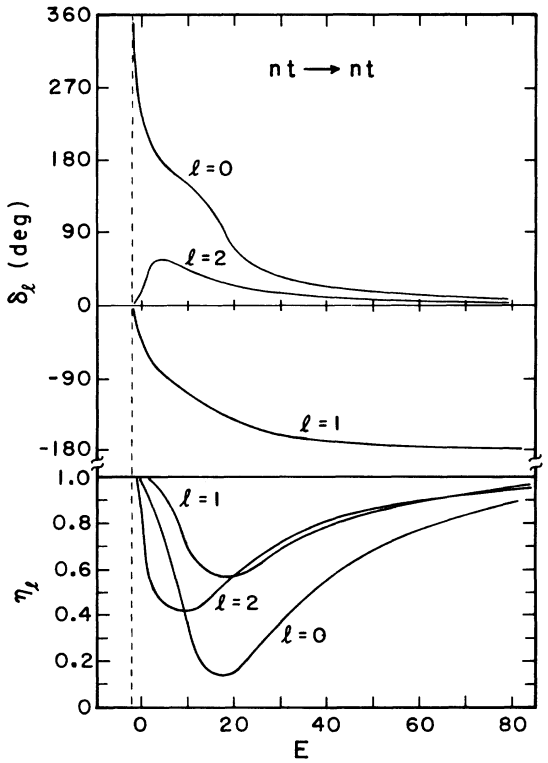

FIG. 12. δ and η versus energy for the $nt \to nt$ for various l with $Z_d = Z_t = 0$ and $\beta_d = \beta_t = 4.0$. The energy units are the same as in Fig. 10.

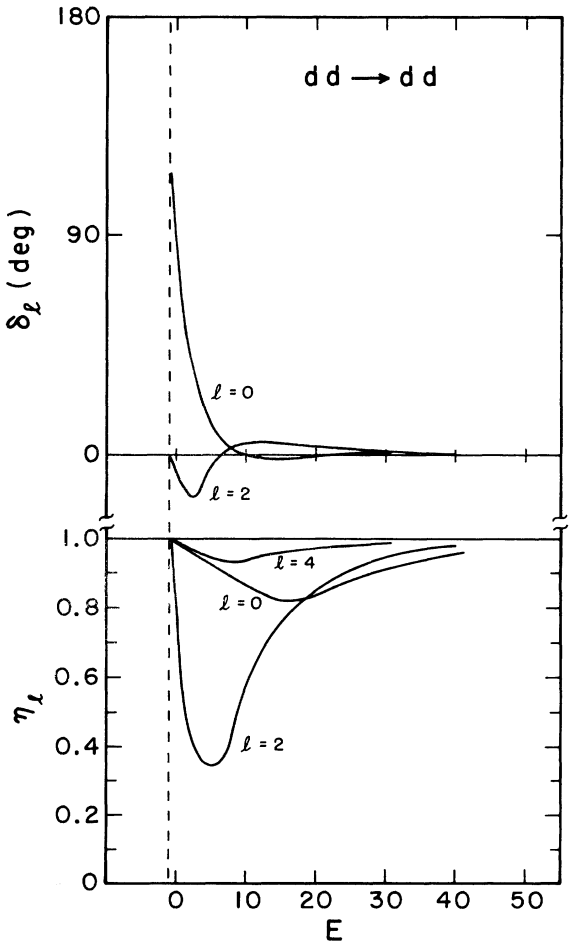

FIG. 13. δ and η versus energy for $dd \to dd$ for various l with $Z_d = Z_t = 0$ and $\beta_d = \beta_t = 4.0$. The energy units are the same as in Fig. 10.

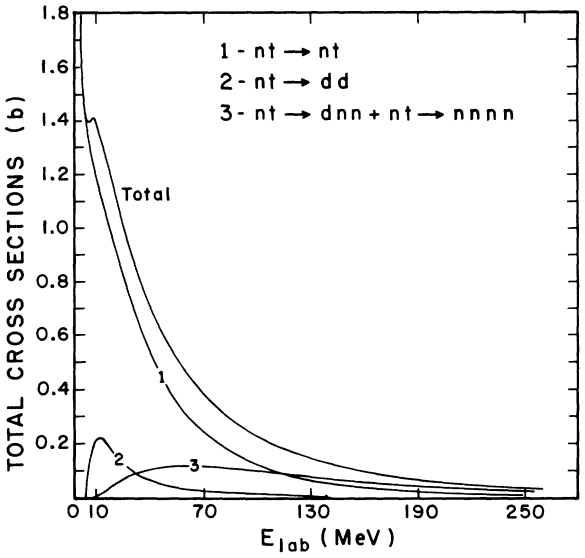

FIG. 14. Total cross sections versus E_n for processes initiated by nt with $Z_d = Z_t = 0$ and $\beta_d = \beta_t = 4.0$.

tions, but it is reassuring that we can reproduce such data within the same order of magnitude.

In spite of the absence of spin and isospin we will also compare our results for the differential cross sections with the four-nucleon data. Both ϵ_d and ϵ_t have already been fixed at the deuteron and triton binding energies. The range parameter β_d of the two-body vertex function was fixed at 3.04 which with $Z_d = 0$ makes the two-body results arising from the solution of Eq. (2) fit the triplet scattering length for nucleon-nucleon scattering. With $Z_t = 0$ and $\beta_t = 7.0$, the nd phase shift calcula-

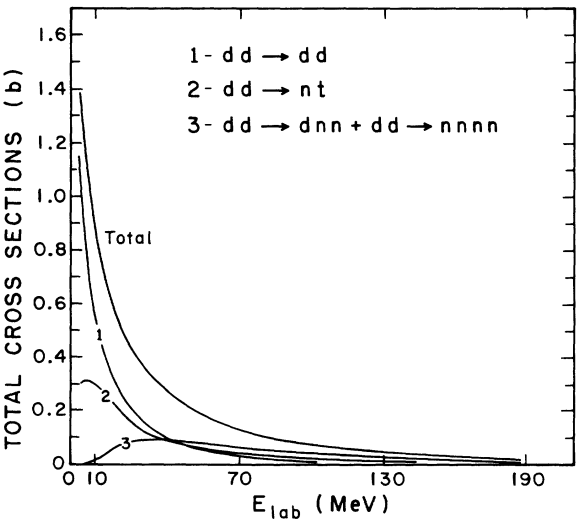

FIG. 15. Total cross sections versus E_d for processes initiated by dd with $Z_d = Z_t = 0$ and $\beta_d = \beta_t = 4.0$.

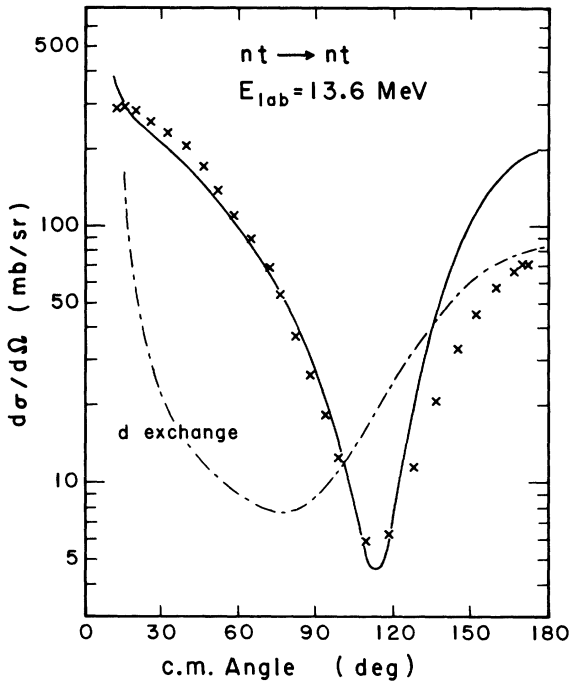

FIG. 16. Angular distribution for $nt \to nt$ at $E_n = 13.6$ MeV with $Z_d = Z_t = 0$, $\beta_d = 3.04$, and $\beta_t = 7.0$. The solid line results from the exact solution of Eq. (6) and the dash-dotted line the result one obtains when only d-particle exchange is included. The crosses are experimental points from Ref. 14.

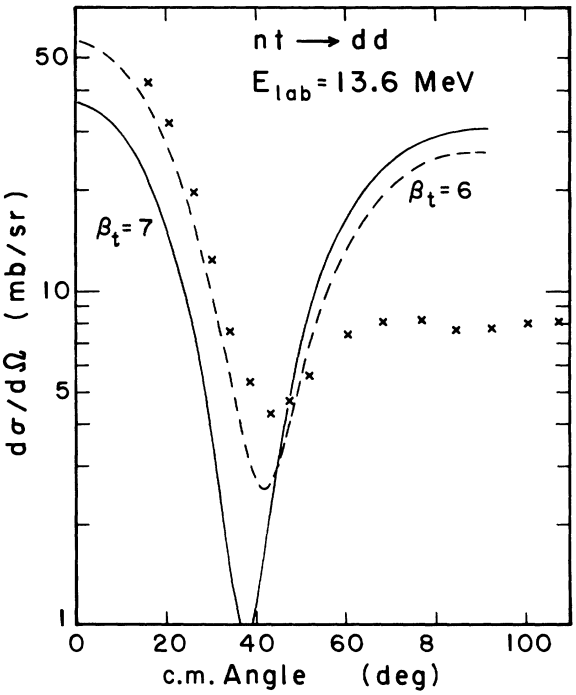

FIG. 17. Angular distribution for $nt \to dd$ at $E_n = 13.6$ MeV with $Z_d = Z_t = 0$, $\beta_d = 3.04$, and two values of β_t. The crosses are experimental points from Ref. 14.

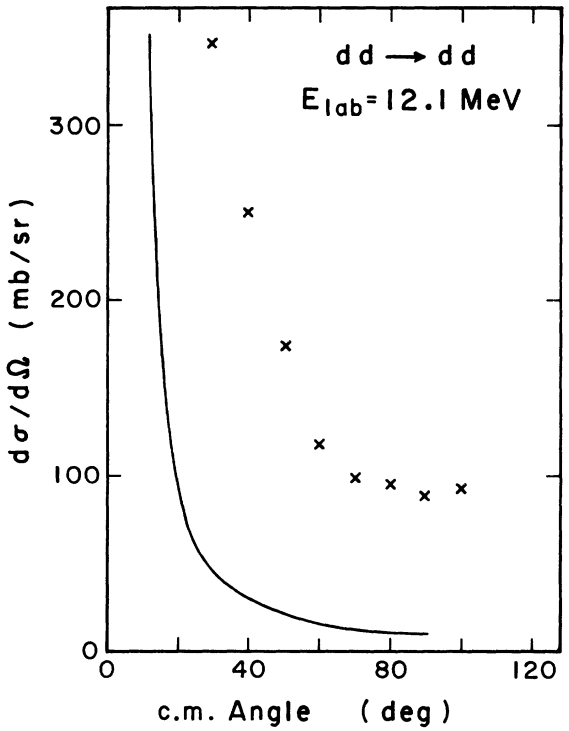

FIG. 18. Angular distribution for $dd \to dd$ at $E_d = 12.1$ MeV with $Z_d = Z_t = 0$, $\beta_d = 3.04$, and $\beta_t = 7.0$. The crosses are experimental points from Ref. 15.

tion resulting from the solution of Eq. (5) gives a reasonably good fit to the $J = \frac{1}{2}$, $l = 0$ neutron-deuteron phase shift analyses.[13] In Figs. 16–18 we display a few results for the elastic and rearrangement differential cross sections for energies above the four-body threshold. In Fig. 16, we show two results. The solid line represents the elastic differential cross section for $nt \to nt$ resulting from the full scattering amplitude as described by Eq. (16) and the dashed line is the cross section one would obtain if only d-particle exchange was present. The difference between the two results gives a clear indication of the importance of two-step processes. Our calculation for $nt \to nt$ and $nt \to dd$ seems to fit the data much better than for dd elastic scattering. Only by introducing spin and isospin corrections to our model can we know if the discrepancies obtained are due to the approximate nature of our three-body amplitude or to the absence of Pauli exclusion effects. The results seem nevertheless encouraging enough to stimulate more exact calculations where both spin and isospin would be included.

V. DISCUSSION

In the previous sections a model four-body problem was introduced and its numerical predictions were examined for a system simulating four nucleons. The four-body equations described in Sec. III were exactly solved but not all possible graphs consistent with both $d \to n + n$ and $t \to d + n$ interactions were included. A few of the simplest omitted diagrams are shown in Fig. 19. In dd scattering we expect that the graphs depicted in Fig. 19(b) may be important since the deuteron is so loosely bound. The absence of these contributions may account for the poor results obtained above for $dd \to dd$ but spin effects may also be important in this reaction.

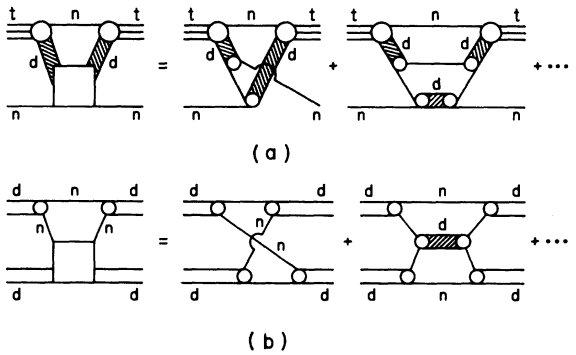

FIG. 19. (a) Some of the omitted diagrams contributing to $nt \to nt$ resulting from virtual nd scattering not involving the t. (b) Some of the omitted diagrams contributing to $dd \to dd$ resulting from virtual nd scattering not involving the t.

With the omission of so many graphs in the model, the lack of unitarity violation in our numerical results may be considered surprising. In Sec. II we outlined an argument for understanding the lack of unitarity violation in the three-body sector, and the argument may be suitably generalized to the four-body case. We consider a more general four-body model containing a sufficient number of nonidentical particles so that the neglected graphs noted above do not appear. A suitable model involves two pairs of identical particles n and n' and the couplings $n + n \to d$ and $n' + n' \to d'$ as well as $n' + d \to t$ and $n + d' \to t'$. The $2 \to 2$ reactions initiated by nt' are then $nt' \to nt'$, $nt' \to n't$, and $nt' \to dd'$. Since there are no particle exchanges present in the three-body sector, no vertex corrections or other such complications arise and the model is exact and analogous to those discussed in our previous work.[7] In this primed model, the Bose symmetry is included only in pairs and is absent in three- or four-particle states. If we now consider the limit of this model as $n' \to n$, $d' \to d$, and $t' \to t$, the model solved in the previous sections is recovered. We expect that the $2 \to 3$ and $2 \to 4$ cross sections obtained in Sec. IV to be in fact identical to the pre-

dictions of a primed model so chosen that the dynamic and kinematic parameters of the primed and unprimed particles are the same. This argument is analogous to that given in the three-body sector and again points out the lack of complete Bose symmetry introduced by our approximation.

As was previously pointed out, *nd* scattering in the model proceeds exclusively in *s* wave through the t. This may be in fact a serious shortcoming of the model since it is known that higher partial waves play an important role in neutron-deuteron scattering, even at low energies. At the present time we have no way to estimate their importance in the four-body sector, although at the expense of simplicity and computer time, we could have generalized the present model to include *nd* scattering in higher partial waves.

It is rather difficult to compare the results of our model with the previous work[6] since we have included no spin and isospin effects. Nevertheless it may be appropriate to compare our method with those used by others. The technique we have used involves a physically based approximation to the three-body amplitude that results in four-body equations that are numerically solved without much difficulty. Our bound state results are not too realistic but in the scattering region our equations yield results that involve no unitarity violation. In contrast to this approach, most other work has involved mathematical approximations in the four-body equations that have so far given solutions at bound state and threshold energies. The four-body binding energies obtained by these methods seem much more realistic than our results but whether these methods can yield unitary answers above the four-body threshold remains to be seen.

The outcome of the calculations we have described in Sec. IV seems to indicate that the results can be considerably improved if both spin and isospin are properly included. The number of coupled equations will then increase by a factor of 3 and the box diagrams will become more complicated since both the spin-triplet and spin-doublet states of the two-nucleon system will appear in all possible combinations. Such a task will probably exceed the present capabilities of our computer but if these difficulties can be overcome, the results of such a calculation will be reported in a later publication.

APPENDIX A: $\tau_d(X)$

The two-particle propagator is discussed in detail elsewhere[8] so that here we just list the results:

$$\tau_d(X)=\frac{S_d(X)}{X}, \tag{A1}$$

$$[S_d(X)]^{-1}=Z_d-\tfrac{1}{2}\gamma_d{}^2 \times\int\frac{d^3n}{(2\pi)^3}\frac{f_d{}^2(\vec{n})}{(2\vec{n}^2+\epsilon_d)(X-\epsilon_d-2\vec{n}^2)}, \tag{A2}$$

$$Z_d=1-\tfrac{1}{2}\gamma_d{}^2\int\frac{d^3n}{(2\pi)^3}\frac{f_d{}^2(\vec{n})}{(2\vec{n}^2+\epsilon_d)^2}. \tag{A3}$$

For the vertex function we have adopted the Hulthén form $f_d(\vec{q})=(\vec{q}^2+\beta_d{}^2)^{-1}$ where β_d is the range parameter. The specific form of the resulting propagator τ_d after all integrals have been analytically performed can be found elsewhere.[9] The n-n interaction is therefore characterized by the binding energy of the d particle ϵ_d, the range parameter β_d, and the wave function renormalization constant Z_d. Once ϵ_d, β_d, and Z_d are fixed the coupling constant γ_d is obtained through (A3).

The unit of energy in our choice of units is equivalent to 4.452 MeV and the unit of length is equal to 2.16 fm.

APPENDIX B: $\tau_t(X)$

We construct the t propagator by summing the series of self-energy bubbles.[8] Graphically the propagator is shown in Fig. 5(b) and the corresponding unrenormalized amplitude is given by

$$\tau_t^{(u)}=\frac{1}{E+\epsilon_t^{(0)}}+\frac{1}{E+\epsilon_t^{(0)}}I(E)\frac{1}{E+\epsilon_t^{(0)}}+\cdots. \tag{B1}$$

We take the bare energy of the t at rest to be $-\epsilon_t^{(0)}$. $I(E)$ represents a bubble involving an n and a fully dressed d, and is given by

$$I(E)=[\gamma_t^{(u)}]^2\int\frac{d^3n}{(2\pi)^3}f_t{}^2(\vec{n})\tau_d(E+\epsilon_d-\vec{n}^{2\frac{2}{3}}). \tag{B2}$$

We have taken the d-particle propagator to be already renormalized. Requiring that $\tau_t^{(u)}$ have a pole at the physical t energy $E=-\epsilon_t$ gives the relation

$$\epsilon_t^{(0)}=\epsilon_t-[\gamma_t^{(u)}]^2\int\frac{d^3n}{(2\pi)^3}f_t{}^2(\vec{n})\tau_d(\epsilon_d-\epsilon_t-\vec{n}^{2\frac{2}{3}}). \tag{B3}$$

Assigning to the renormalized propagator $\tau_t=\tau_t^{(u)}/Z_t$ a unit residue at the pole gives

$$\tau_t(X)=S_t(X)/(X), \tag{B4}$$

where $S_t(X)$ has the form

$$[S_t(X)]^{-1}=Z_t-\frac{\gamma_t{}^2}{X}\times\int\frac{d^3n}{(2\pi)^3}[\tau_d(X+Y)-\tau_d(Y)]f_t{}^2(\vec{n}), \tag{B5}$$

$$X=E+\epsilon_t,$$

$$Y=\epsilon_d-\epsilon_t-\vec{n}^{2\frac{2}{3}}.$$

The wave function renormalization constant Z_t is given by

$$Z_t = 1 + \gamma_t^2 \int \frac{d^3n}{(2\pi)^3} \{YS_d'(Y) - S_d(Y)/Y^2\} f_t^2(\vec{n}) , \tag{B6}$$

where $S_d'(Y)$ indicates the derivative of $S_d(Y)$. γ_t is the renormalized coupling constant given by

$$\gamma_t^2 = Z_t(\gamma_t^{(u)})^2 . \tag{B7}$$

As a vertex function we have chosen $f_t(\vec{n}) = (\vec{n}^2 + \beta_t^2)^{-3}$ in order that the asymptotic behavior of $\langle k' | T_{nd}(E) | k \rangle$ given by Eq. (5) in the limit of $k \to \infty$ and $k \to 0$ be the same as that for the s-wave component of the T matrix described by Eq. (3).[16] The independent parameters that characterize the n-d interaction in the model are, therefore, the binding energy of the t quasiparticle ϵ_t, the range parameter of the vertex function β_t, and the wave function renormalization constant Z_t. Once ϵ_t, β_t, and Z_t are specified, the value of the coupling constant γ_t is fixed through Eq. (B6).

---

*Supported in part by the National Science Foundation under Grant No. GP-32167X.

†Supported by Instituto de Alta Cultura, Portugal. Present address: University of Maryland, College Park, Maryland 20742.

[1]See for example, Y. E. Kim and A. Tubis, Annu. Rev. Nucl. Sci. 24, 69 (1974).

[2]O. A. Yakubovskii, Yad. Fiz. 5, 1312 (1967) [Sov. J. Nucl. Phys. 5, 937 (1967)]; P. Grassberger and W. Sandhas, Nucl. Phys. B2, 181 (1967), and references contained therein.

[3]V. F. Kharchenko and V. E. Kuzmichev, Phys. Lett. 42B, 328 (1972); I. M. Narodetskii, E. S. Galpern, and V. N. Lyakhovitsky, *ibid.* 46B, 51 (1973).

[4]V. F. Kharchenko and V. P. Levashev, Phys. Lett. 60B, 317 (1976).

[5]J. A. Tjon, Phys. Lett. 56B, 217 (1975).

[6]M. Sawicki and J. M. Namyslowski, Phys. Lett. 60B, 331 (1976); E. O. Alt, P. Grassberger, and W. Sandhas, Phys. Rev. C 1, 85 (1970).

[7]A. C. Fonseca and P. E. Shanley, Phys. Rev. D 13, 2255 (1976).

[8]R. D. Amado, Phys. Rev. 132, 485 (1963).

[9]R. Aaron, R. D. Amado, and Y. Y. Yam, Phys. Rev. 136, B650 (1964).

[10]This problem has been solved by J. B. Bronzan [Phys. Rev. 139, B751 (1965)] for the extended Lee model.

[11]J. H. Hetherington and L. H. Schick, Phys. Rev. 137, B935 (1965).

[12]A. M. Sourkes, A. Houdayer, W. T. H. van Oers, R. F. Carlson, and R. E. Brown, Phys. Rev. C 13, 451 (1976).

[13]W. T. H. van Oers and K. W. Brockman, Nucl. Phys. A92, 561 (1967).

[14]J. L. Detch, R. L. Hutson, N. Jarmie, and J. H. Jett, Phys. Rev. C 4, 52 (1971).

[15]A. S. Wilson, M. C. Taylor, J. C. Legg, and G. C. Phillips, Nucl. Phys. A126, 193 (1969).

[16]A. Alessandrini and R. L. Omnes, Phys. Rev. 139, B167 (1965).